HAYATI
Journal of Biosciences

Vol. 33 No. 2, March 2026 331-344
DOI:10.4308/hjb.33.2.331-344
ISSN: 1978-3019
EISSN: 2086-4094

Research Article

Check for updates

OPEN ACCESS

Transcriptomic Dissection of Long-Juvenility in Soybean: A Comparative Study of Grobogan Cultivar and Its Derivative Long Juvenile AP18 Line

Habib Rijzaani, I Made Tasma*

Research Center for Food Crops, National Research and Innovation Agency (BRIN). Bogor Regency 16915, Indonesia

ARTICLE INFO

Article history:
Received September 3, 2025
Received in revised form September 19, 2025
Accepted October 15, 2025
Available Online November 10, 2025

KEYWORDS:
developmental regulation,
differential expression,
long juvenility,
RNA-seq,
soybean

ABSTRACT

The long juvenile (LJ) trait in soybean extends the vegetative phase, enabling cultivation in low-latitude regions. This study investigated transcriptomic differences between the Grobogan cultivar (control) and the AP18 (LJ) soybean line using RNA-seq. Young leaf tissues from plants at the vegetative stage were collected under field conditions and sequenced using the Illumina NovaSeq 6000 platform. After quality filtering and alignment to the soybean reference genome, 24,716 expressed transcripts were retained for analysis. Differential expression analysis identified 5,005 upregulated and 4,534 downregulated transcripts in AP18 relative to Grobogan. Functional enrichment analysis revealed the upregulation of genes involved in ribosome biogenesis and secondary metabolism, and the downregulation of genes related to photosynthesis and energy metabolism. While known LJ-related genes FT2A (E9) and ELF3B (J) showed differential expression, the magnitude was modest. These findings highlight widespread transcriptomic reprogramming associated with the LJ trait, providing insight into potential pathways that influence juvenile phase extension.

1. Introduction

Soybeans (*Glycine max* [L.] Merr.) are a valuable crop worldwide, renowned for their protein-rich seeds and their contribution to sustainable agriculture through biological nitrogen fixation. The growth cycle of the plant, particularly the transition from the vegetative to the reproductive stage, is tightly controlled by genetic and environmental factors, such as photoperiod, temperature, and hormone signaling (Tasma *et al*. 2001; Tasma *et al*. 2003; Cao *et al*. 2016; Gong 2020). Among them, the juvenile period—the period prior to a plant's responsiveness to floral inducers—is an important developmental phase that regulates soybean adaptability and yield potential under different environments.

In tropical and equatorial climates where short-day conditions persist throughout the year, soybean cultivars possessing the long juvenility (LJ) trait are especially useful. The LJ trait delays flowering initiation under inductive conditions, enabling more vegetative growth, greater biomass accumulation, and improved yield stability (Hartwig & Kiihl 1979; Li *et al*. 2024). Introgression of the LJ trait into elite lines has been employed to convert temperate soybean germplasm for use in tropical ecosystems, particularly in Southeast Asia and Africa (Tasma *et al*. 2018; Han *et al*. 2021).

Grobogan is one such superior cultivar that was developed and launched in Indonesia for its desirable

*Corresponding Author
E-mail Address: i.made.tasma@brin.go.id

agronomic traits of high yield, earliness, large seed size, and extensive adaptation to local environments (Suhartina *et al*. 2022; Fattah *et al*. 2024). It has been extremely popular among farmers and is used as a recurrent parent in breeding programs aimed at improving stress tolerance and yield (Utomo *et al*. 2018; Soehendi *et al*. 2024). Improved lines developed from Grobogan have been established to carry the long juvenile trait, resulting in better performance in tropical latitudes (Tasma *et al*. 2018).

While a few flower-associated soybean genes - e.g., E1, GmFTs, and Tof11/12 - have been characterized for their roles in photoperiod sensitivity and flowering time (Tasma *et al*. 2001; Lu *et al*. 2020; Lv *et al*. 2022), the transcriptomic underpinnings of the long juvenility trait are still an active area of research. Genome-wide contrasts in gene expression between LJ and non-LJ genotypes have been investigated in limited studies, especially under field-grown conditions where stress response and developmental plasticity also play a role (Wu *et al*. 2019; Yue *et al*. 2021).

In the present research, we conducted comparative RNA sequencing (RNA-seq) analysis of young leaf tissue samples collected before flowering in field-grown Grobogan cultivar and an advanced line with long juvenile genes, AP18 (Tasma *et al*. 2018). Our objective was to identify differentially expressed genes (DEGs) and overrepresented biological pathways that may underlie the long juvenility trait in soybean. The present research provides insights into the molecular architecture of flowering delay and can guide future breeding strategies for tropical adaptation.

2. Materials and Methods

2.1. Plant Materials

Plant materials used in this study consisted of the Grobogan soybean cultivar (control) and the AP18 line, which was derived from a cross between Grobogan and an introduced line carrying the long-juvenile (LJ) trait (Tasma *et al*. 2018). Plants were grown under natural field conditions at the Field Experiment Station, Citayam, Depok, West Java. Young leaves were harvested from plants at the vegetative stage in February 2024, with three biological replicates per genotype. Collected leaves were immediately frozen in liquid nitrogen and stored at -80 °C until RNA extraction.

2.2. RNA Library Preparation

Total RNA was extracted and used for RNA-Seq library preparation with the Collibri™ Stranded RNA Library Prep Kit for Illumina Systems (Cat# A38996096, Thermo Fisher Scientific), following the manufacturer's instructions (Thermo Fisher Scientific 2020). For each sample, 1 µg of high-quality RNA was enzymatically fragmented prior to cDNA synthesis. End-repair, A-tailing, and adapter ligation were followed by PCR amplification to enrich cDNA fragments and incorporate dual indices. Libraries were quantified using a Qubit Fluorometer, and their fragment sizes were assessed using an Agilent TapeStation system. Quantitative PCR (qPCR) was used for final quantification. Pooled libraries were sequenced on an Illumina NovaSeq 6000 platform using 300-cycle paired-end (PE150) chemistry. Genetika Science, Jakarta, Indonesia, conducted sequencing.

2.3. RNA-Seq Data Preprocessing

Raw paired-end RNA-Seq reads were subjected to a series of quality filtering steps. Adapter sequences and low-quality bases were trimmed using AdapterRemoval v2 (Schubert *et al*. 2016) and fastp (*Chen et al*. 2018), and ribosomal RNA contamination was removed using RiboDetector (Deng *et al*. 2022). Clean reads, ranging from 12 to 23 million per sample, were retained for downstream analysis.

2.4. Read Alignment to Reference Genome

Filtered reads were mapped to the soybean reference genome (Glycine max Wm82.a4.v1, SoyBase release V4) (Schmutz *et al*. 2010) using the STAR aligner (v2.7.10a) (Dobin *et al.* 2012) with two-pass mode enabled to improve detection of splice junctions. The alignment performance was recorded, including the total number of mapped reads and the proportion of uniquely mapped reads.

2.5. RNA-Seq Quality Assessment

Comprehensive quality assessments of the mapped reads were performed using RSeQC (v4.0.0) (Wang *et al*. 2012). Splice junction saturation analysis (junction_saturation.py) was used to evaluate transcriptome completeness and sufficiency of sequencing depth. GC content distribution was assessed to detect compositional bias, with the average GC content compared to that of known soybean coding regions. Gene body coverage

analysis (geneBody_coverage.py) was used to examine read coverage bias along transcript lengths. These combined assessments ensured the suitability of the RNA-Seq data for expression-level analyses.

2.6. Transcriptome Diversity and Expression Saturation

Transcriptome variation and sequencing saturation were assessed using DESeq2 (v1.38.0) (Love *et al*. 2014). Variance-stabilized expression values were used for hierarchical clustering and visualization of sample grouping based on transcriptomic similarity. Additionally, RPKM-based expression saturation analysis was conducted by subsampling transcriptomic reads and comparing RPKM estimates at different depths to evaluate whether sequencing coverage was adequate for robust expression quantification.

2.7. Differential Gene Expression Analysis

Expression values in RPKM format were analyzed using edgeR (Robinson *et al*. 2009) to identify differentially expressed genes (DEGs) between the Long Juvenile (LJ) soybean line and the Grobogan cultivar. The top 500 DEGs were used for heatmap-based clustering analysis, while principal component analysis (PCA) was employed to visualize sample grouping based on global expression patterns. Filtered expression values were normalized by transcriptome library size prior to differential expression testing using the limma (Ritchie *et al*. 2015) package with a linear model. For each gene, the model estimated group-wise means and variances of expression. Significantly differentially expressed genes were visualized using a volcano plot.

2.8. GO Enrichment and KEGG Pathway Analysis

Gene Ontology (GO) enrichment analysis using the AnnotationHub R package (Morgan & Shepherd 2024) was conducted to identify biological processes, molecular functions, and cellular components significantly enriched among the DEGs. In parallel, KEGG (Kyoto Encyclopedia of Genes and Genomes) pathway analysis (Kanehisa *et al*. 2022) was employed to identify metabolic and signaling pathways that were overrepresented among differentially expressed genes. These enrichment analyses provided insights into the functional implications of transcriptional changes between the AP18 LJ line and that of the non-LJ Grobogan variety.

3. Results

3.1. RNA Sequencing Output and Quality

A total of six RNA-seq libraries were generated, consisting of three biological replicates each for the AP18 and Grobogan genotypes. Sequencing on the Illumina NovaSeq 6000 platform yielded between 49.72 and 125.43 million paired-end reads per sample. All libraries exhibited high base quality, with over 85% of reads per sample exceeding Q30 and around 90% surpassing Q20 in most cases. Detailed sequencing statistics are presented in Table 1.

3.2. Quality Filtering and Read Mapping

After adapter and quality trimming with AdapterRemoval and fastp, and ribosomal RNA removal using RiboDetector, between 12 and 23 million clean reads per sample were retained, representing approximately 20%–30% of total reads. These clean reads were mapped to the soybean reference genome (Wm82.a4.v1) using STAR, with an average overall mapping rate of approximately 99%. Of the mapped reads, about 66% to 80% were uniquely aligned to the genome. Mapping details for each sample are shown in Table 2.

3.3. Transcriptome Saturation and Mapping Bias

Saturation analysis using RSeQC revealed that all samples achieved near-complete detection of exon–intron junctions, indicating an adequate sequencing depth (Figure 1). Graphs of the known junctions are nearly stable at high sampling values for all samples, whereas novel junctions are still slightly increasing. The similar

Table 1. Summary of RNA-seq read quality and output per sample of Grobogan and AP18 plants

Sample name	Total reads (M)	Total bases (Gb)	Bases >Q20 (%)	Bases >Q30 (%)
AP18 – I	57.25	8.65	91.39	85.66
AP18 – II	78.17	11.80	85.50	78.57
AP18 – III	49.72	7.51	88.71	82.60
Grobogan – I	59.26	8.95	91.25	85.66
Grobogan – II	74.07	11.18	89.22	83.31
Grobogan – III	125.43	18.94	91.40	86.00

Table 2. Summary of RNA-seq read mapping statistics for each sample against the soybean reference genome

Sample	AP18-1	AP18-2	AP18-3	Grobogan-1	Grobogan-2	Grobogan-3
Clean input sequence number	20,861,077	16,753,618	15,317,047	15,418,385	12,097,514	23,543,476
% Uniquely mapped reads	78.42	69.84	70.44	66.18	80.15	76.50
Average mapped length (bp)	270.14	249.8	246.66	240.22	259.67	248.01
% of reads mapped to multiple loci	21.17	29.76	29.15	32.68	18.83	22.32
% of reads unmapped	0.42	0.40	0.42	1.14	1.02	1.18

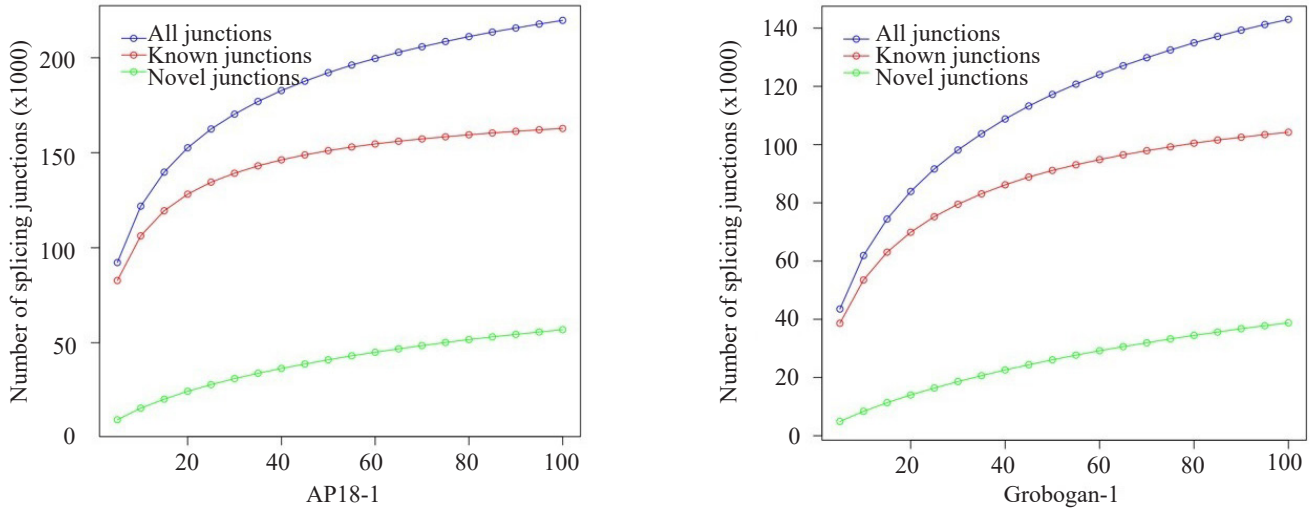

Figure 1. Splice junction saturation analysis of RNA-seq data from representative samples of Grobogan and AP18 genotypes. The X-axis shows the percentage of total mapped reads, and the Y-axis indicates the number of detected splice junctions (×1000). Blue lines represent all junctions, red lines denote known (annotated) junctions, and green lines indicate novel (unannotated) junctions. Representative samples are shown; all replicates exhibited comparable patterns

saturation curves between genotypes suggest that sufficient sequencing depth is achieved for the reliable detection of exon–intron junctions. The GC content distribution of the reads showed an average of ~41%, which is slightly lower than the expected 42-44% GC contents in soybean coding regions (Figure 2). Gene body coverage analysis demonstrated a 3′ end bias across most samples, with read density gradually increasing from the 5′ end, peaking around the 90th percentile of gene length, then decreasing (Figure 3). One AP18 sample showed a minor deviation from this general trend. The slight discrepancy in GC content may result from a 3′ bias in read coverage, which is common in poly(A)-based RNA-seq, as it concentrates reads from typically lower-GC 3′ UTRs. However, this bias is largely consistent among the samples and should not affect the differential expression analysis.

3.4. Transcriptome Diversity and Expression Saturation

Transcript-level expression data were analyzed using DESeq2 to compute pairwise similarities among samples. Clustering analysis reveals a clear grouping of samples according to genotype: Grobogan control group (Grob_1, _2, _3) and AP18 long-juvenile group (AP_1, _2, _3). Sample AP_1 and Grob_1 exhibit slight deviations from their respective groups, but overall clustering is consistent with the expected genotype-based classification. (Figure 4).

3.5. Differential Expression Between AP18 and Grobogan

Based on transcriptome mapping to the soybean reference genome, a total of 58,986 transcripts were

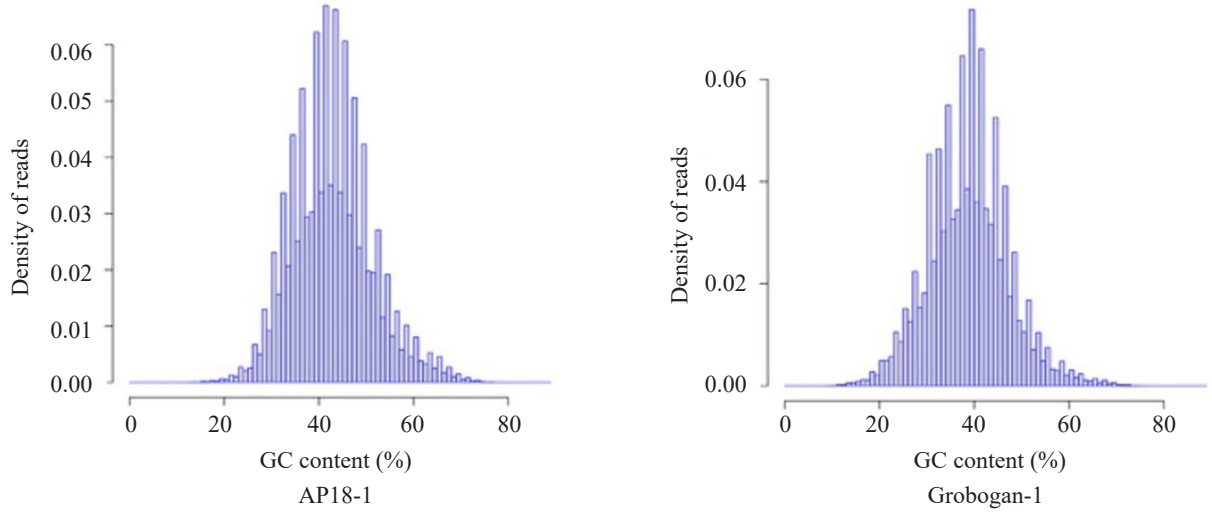

Figure 2. GC content distribution of RNA-seq reads from representative samples of Grobogan and AP18 genotypes. The X-axis indicates the GC content (%) of sequencing reads, and the Y-axis shows the density of reads at each GC content level. The histograms display a unimodal distribution centered around ~41% GC content for both genotypes. Patterns were consistent across all replicates

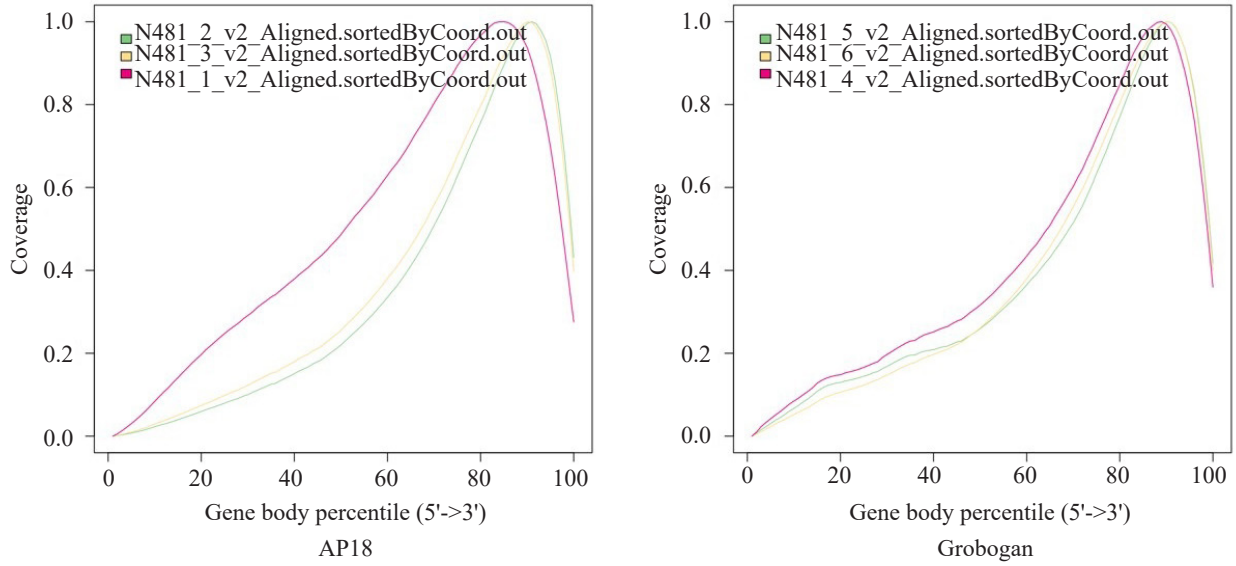

Figure 3. Gene body coverage distribution of RNA-seq reads from representative samples of Grobogan and AP18 genotypes. The X-axis represents the gene body percentile from 5′ to 3′ end, and the Y-axis shows normalized read coverage (0–1 scale). Both samples exhibit a 3′ coverage bias, with read density increasing toward the 3′ end and peaking near the 90th percentile of gene length

initially detected across all samples. Transcripts with low expression levels - defined as having less than 0.5 counts-per-million (CPM) in at least two samples - were excluded from downstream analysis. This filtering step resulted in the retention of 24,716 transcripts for further evaluation.

The filtered transcript expression data were normalized by accounting for library size differences among samples. Differential gene expression (DEG) analysis was then conducted using the limma package with a linear modeling approach. This method estimated both group-level average expression (LJ vs. Control) and gene-specific variance. Statistical testing identified 5,005 transcripts that were significantly upregulated and 4,534 transcripts that were significantly downregulated in the LJ (AP18) plants compared to the control (Grobogan). In comparison, 15,177 transcripts showed no significant changes in expression.

To visualize the differential expression landscape, two complementary plots were generated (Figure 5).

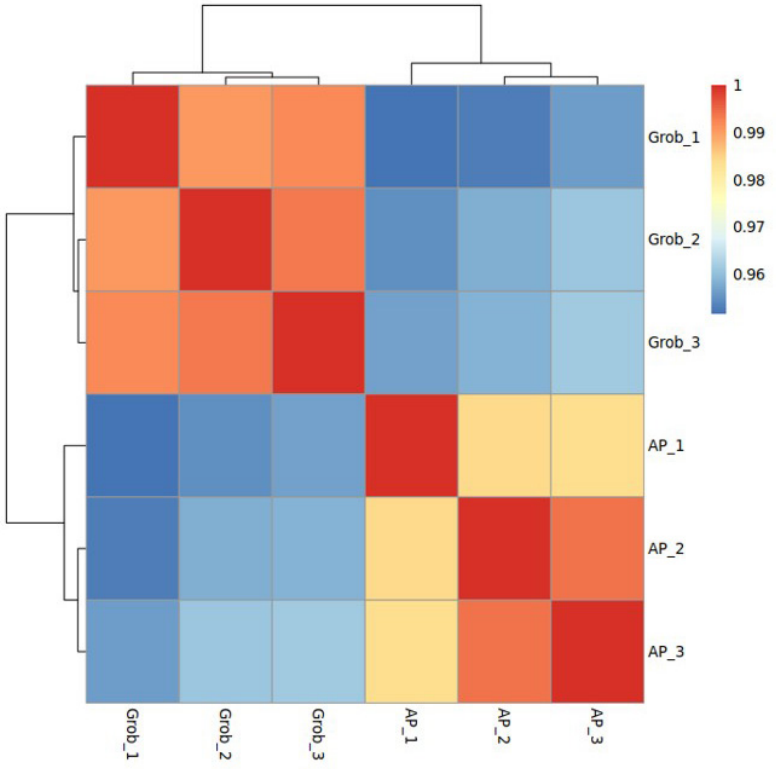

Figure 4. Heatmap of transcriptome profile similarity and hierarchical clustering among RNA-seq samples. The Blue–White–Red color scale represents similarity values, with blue indicating lower similarity, white indicating intermediate, and red indicating high similarity

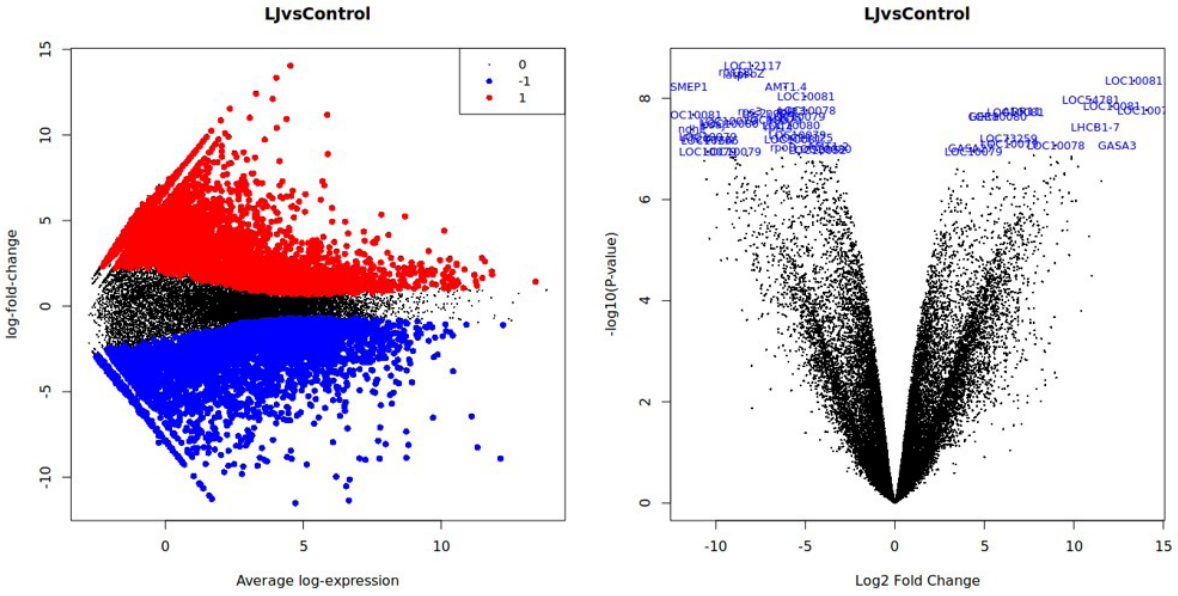

Figure 5. Differential expression analysis between long-juvenile (LJ) and control (Grobogan) soybean lines. (Left panel) MD plot showing the relationship between average log-expression (X-axis) and log fold-change (Y-axis) for all genes. Red dots represent significantly upregulated genes in the LJ line, while blue dots represent down-regulated genes. (Right panel) Volcano plot illustrating transcript-level differential expression, with $\log_2$ fold change on the X-axis and $-\log_{10}$(P-value) on the Y-axis. Significantly upregulated genes are highlighted in red, while downregulated genes are highlighted in blue. The top 20 most differentially expressed genes are labeled in blue

The MD plot shows the average log-expression of each gene against its log fold-change (logFC), highlighting genes with the strongest up- and downregulation patterns. The volcano plot displays the log2 fold change against the –log10 P-value, emphasizing genes that are both highly differentially expressed and statistically significant. Upregulated genes are marked in red, and downregulated genes are marked in blue. The top 20 most radically expressed genes are annotated by name. Both plots were generated using edgeR and limma to identify statistically significant differences in expression between the two genotypes.

Following gene annotation and expression normalization using the edgeR and limma pipelines, the top 20 differentially expressed genes (DEGs) between the long-juvenile (LJ) line (AP18) and the control Grobogan cultivar were identified based on log fold change (logFC) and average expression (AveExpr) values. These genes exhibit the most significant transcriptional divergence between the two genotypes and are presented in Table 3.

Among the top 20 differentially expressed genes (DEGs), 16 were significantly down-regulated in the long-juvenile (LJ) soybean line, with logFC values ranging from –4.92 to –10.14, while four were upregulated (logFC +4.94 to +7.06). The majority of down-regulated genes were functionally associated with photosynthesis, ribosome biogenesis, and nutrient transport. These included photosynthetic electron transport components such as psbZ (Photosystem II reaction center Z protein), psbD2 (Photosystem II protein D2), psa9 (Photosystem I subunit IX), cytochrome f, and the 49 kDa subunit of NADH dehydrogenase. Several ribosomal proteins (30S S2, S3, S18; 50S L14, L33) and translation factors (e.g., eukaryotic translation initiation factor 5B) were also strongly suppressed, suggesting reduced protein synthesis activity. In addition, nutrient-related transporters such as sucrose transporter SUC8 and ammonium transporter AMT1.4, together with the RNA processing regulator DEAD-box ATP-dependent RNA helicase 36, were significantly down-regulated.

In contrast, four genes were consistently upregulated in the LJ line, including multiple members of the germin-like protein family and an AAI_LTSS superfamily protein. Germin-like proteins are typically associated with redox activity, stress responses, and early developmental processes, suggesting a potential reprogramming of stress and signaling mechanisms in LJ plants.

To further investigate transcriptomic differences between the long-juvenile (LJ, AP18) and control (Grobogan) soybean plants, expression values in RPKM for each gene were analyzed using the edgeR package. The top 500 genes with the most significant differential expression between the two genotypes were selected for hierarchical clustering analysis. The resulting heatmap revealed a clear separation between the two sample groups, with AP18 and Grobogan forming distinct clusters based

Table 3. Top 20 differentially expressed genes between the long-juvenile (AP18) and control (Grobogan) soybean lines

Entrezid	Symbol	Gene name	LogFC	AveExpr
3989281	psbZ	photosystem II reaction center Z protein	-8.06	7.99
121173225	LOC121173225	cytochrome f	-7.96	6.08
3989295	atpI	ATPase IV subunit	-8.86	8.73
3989320	rps18	30S ribosomal protein S18	-8.98	7.25
100797759	AMT1.4	ammonium transporter AMT1.4	-6.12	6.51
100814875	LOC100814875	eukaryotic translation initiation factor 5B	-4.99	7.52
100786411	LOC100786411	sucrose transport protein SUC8	-4.92	7.05
3989319	rpl33	ribosomal protein L33	-5.83	6.49
3989335	rps3	30S ribosomal protein S3	-8.12	8.82
3989294	rps2	30S ribosomal protein S2	-7.87	7.72
100500326	GER8	germin-like protein	4.94	6.51
100798597	LOC100798597	DEAD-box ATP-dependent RNA helicase 36	-5.50	6.08
100800387	LOC100800387	germin-like protein	5.73	6.05
547928	ADR11	AAI_LTSS superfamily protein	7.06	5.76
3989284	psbD	photosystem II protein D2	-6.42	6.33
3989355	ndhH	NADH dehydrogenase 49 kDa subunit	-6.41	4.77
100806895	LOC100806895	plastid-lipid-associated protein, chloroplastic	-5.82	5.30
100816355	LOC100816355	germin-like protein	6.74	4.62
3989333	rpl14	50S ribosomal protein L14	-6.50	5.56
3989318	psaJ	photosystem I subunit IX	-10.14	6.68

Genes are ranked by P-values of calculated fold-changes (logFC), with associated gene identifiers (ENTREZID), gene symbols (SYMBOL), full gene names (GENENAME), and average expression (AveExpr), which are indicated in bold if expressions are upregulated in LJ lines

on their gene expression profiles. This clustering pattern supports the biological grouping of samples and reflects consistent transcriptomic differences associated with the LJ trait (Figure 6).

Among the top 500 genes, approximately 60% showed up-regulation in the LJ line, indicating increased expression levels compared to the control. The remaining 40% were down-regulated in the LJ samples. These changes in gene expression suggest that the long-juvenile trait is associated with broad transcriptional reprogramming, potentially influencing physiological and developmental processes relevant to flowering time and vegetative growth.

3.6. KEGG Pathway Enrichment Analysis

To investigate the biological functions affected in the LJ line, KEGG pathway enrichment analysis was performed. As shown in Table 4, several pathways showed a significant overrepresentation of down-regulated genes, including ribosome biogenesis in eukaryotes, zeatin biosynthesis, isoflavonoid biosynthesis, the biosynthesis of various plant secondary metabolites, and the MAPK signaling pathway in plants. These results point to reduced cellular activities related to protein synthesis, cytokinin-mediated developmental regulation, and secondary metabolite production. The suppression of MAPK signaling is consistent with developmental modulation associated with delayed flowering and extended vegetative growth under short-day conditions.

In contrast, pathways with a significant overrepresentation of upregulated genes included photosynthesis and related processes (e.g., antenna proteins, porphyrin metabolism, fructose and mannose metabolism), lipid and sugar metabolism (e.g., fatty acid biosynthesis and metabolism, starch and sucrose metabolism, nucleotide sugar metabolism), and structural or transport functions (e.g., motor proteins, cutin/suberin/wax biosynthesis, phagosome, glycan degradation). These findings indicate enhanced photosynthetic capacity, energy storage, and structural metabolism in LJ plants at the vegetative stage, consistent with their prolonged vegetative growth and potential for greater biomass accumulation.

3.7. Expression Profiles of Known Genes Related to Long Juvenile Trait

To assess the involvement of known genes associated with the long juvenile (LJ) trait in soybean, expression

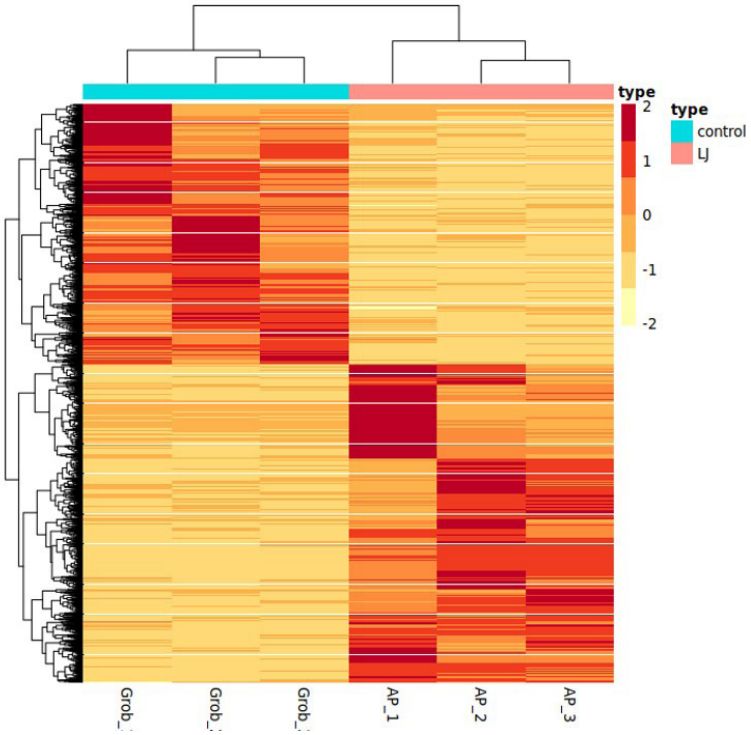

Figure 6. Heatmap showing hierarchical clustering of the top 500 differentially expressed genes between long-juvenile (AP18) and control (Grobogan) soybean lines. Gene expression values are represented as row Z-scores ranging from 2 (light orange) to +2 (dark orange). Each column represents a biological replicate, and each row represents a gene. The clustering pattern separates AP18 from Grobogan samples, with approximately 60% of genes upregulated in AP18 and 40% down-regulated

Table 4. Summary of KEGG pathways enriched among differentially expressed genes in long-juvenile (LJ) soybean line compared to control

Pathway	N	Up	Down	P.up	P.down
Motor proteins	114	62	13	8.10E-16	9.84E-01
Photosynthesis - antenna proteins	33	27	0	5.38E-14	1.00E+00
Amino sugar and nucleotide sugar metabolism	166	62	13	2.56E-07	1.00E+00
Photosynthesis	100	42	29	5.94E-07	6.15E-03
Fructose and mannose metabolism	87	38	3	6.18E-07	1.00E+00
Porphyrin metabolism	76	34	8	1.21E-06	9.78E-01
Fatty acid biosynthesis	44	23	4	2.42E-06	9.72E-01
Metabolic pathways	2453	579	392	1.02E-05	9.99E-01
Biosynthesis of nucleotide sugars	124	46	6	1.05E-05	1.00E+00
Lipoic acid metabolism	45	21	1	6.05E-05	1.00E+00
Ribosome biogenesis in eukaryotes	104	1	35	1.00E+00	1.37E-04
Starch and sucrose metabolism	157	51	23	2.06E-04	9.07E-01
Zeatin biosynthesis	26	5	13	6.29E-01	2.47E-04
Fatty acid metabolism	71	27	5	4.18E-04	9.98E-01
Isoflavonoid biosynthesis	29	1	13	9.99E-01	9.31E-04
Cutin, suberine, and wax biosynthesis	25	12	4	1.71E-03	6.99E-01
Phagosome	108	35	6	1.98E-03	1.00E+00
Biosynthesis of various plant secondary metabolites	35	7	14	5.82E-01	2.28E-03
MAPK signaling pathway - plant	168	17	46	1.00E+00	2.49E-03
Other glycan degradation	27	12	1	3.83E-03	9.96E-01

Downregulated KEGG pathways are shown in bold

levels of FT2A (E9) and ELF3B (J) were examined in the transcriptome dataset. Both genes were detected among the differentially expressed genes (DEGs), although the magnitude of expression change between the LJ line (AP18) and the control variety (Grobogan) was relatively modest. FT2A (E9), a gene previously implicated in delayed flowering under short-day conditions, exhibited a slight reduction in expression in AP18 compared to Grobogan. Conversely, ELF3B (J), which also plays a role in photoperiod sensitivity and flowering time regulation, showed a minor increase in expression in AP18 plants. These patterns are visualized in Figure 7, which shows the normalized expression levels of both genes across all biological replicates. Other known genes previously reported to be associated with the long juvenile trait in soybean did not display significant differential expression in this study, suggesting that their transcriptional activity may not be altered at the vegetative growth stage under the field conditions applied in this experiment.

4. Discussion

This study presents the first comprehensive transcriptomic comparison of the LJ soybean line AP18 and the Grobogan cultivar, providing insight into the molecular basis of the LJ phenotype. The high sequencing depth and quality, together with good mapping statistics, provided comprehensive transcriptome coverage, enabling the confident identification of differentially expressed genes (DEGs). The saturation analysis confirmed sufficient sequencing depth to capture the majority of expressed splice junctions, consistent with earlier research on RNA-seq data quality (Mortazavi *et al*. 2008; Wang *et al*. 2012).

4.1. Transcriptomic Differences and Functional Implications

The transcriptome profiles are neatly clustered by genotype, showing substantial transcriptional divergence between the LJ and control lines. Among the top 500 DEGs identified using edgeR, approximately 60% were upregulated in AP18, reflecting extensive transcriptional reprogramming associated with delayed flowering and prolonged vegetative growth.

Notably, the subset of top 20 DEGs revealed a prevalence of downregulated genes in the LJ line involved in photosynthesis and ribosomal protein biosynthesis. Downregulation of these genes may be an indication of reduced photosynthetic activity and altered protein biosynthesis machinery, which may be linked to developmental adaptations during the extended juvenile phase. Conversely, several of the upregulated genes belonged to the germin-like protein family, whose members are implicated in stress responses and regulation of development in plants (Govindan *et al*. 2024). The differential concerted expression of these

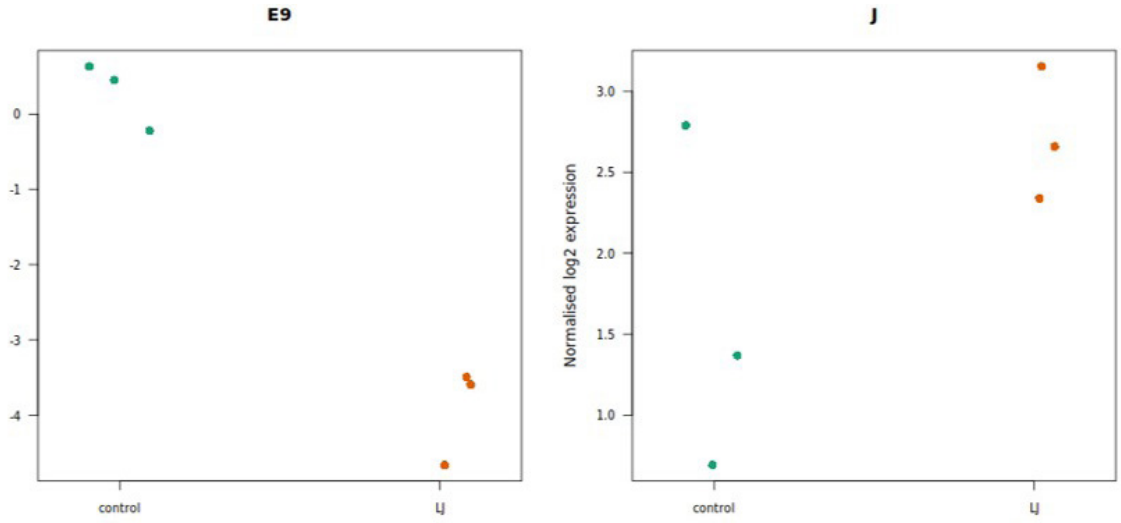

Figure 7. Expression levels of FT2A (E9) and ELF3B (J) genes in control (Grobogan) and long juvenile (AP18) soybean lines. Expression is shown as normalized counts across three biological replicates per genotype. FT2A exhibits a slight down-regulation in AP18, while ELF3B shows a modest increase

gene sets indicates metabolic readjustments and stress adaptation mechanisms that confer the LJ trait.

Similar to our findings, drought-stress transcriptome profiling in Iris germanica revealed strong downregulation of photosynthesis- and ribosome-related genes, indicating reduced metabolic activity under stress-induced developmental delay (Zhang *et al*. 2021). Likewise, a time-series RNA-seq study of Paulownia tomentosa under short-day treatment highlighted coordinated suppression of carbon fixation and photosynthetic pathways during growth cessation (Wang *et al*. 2019).

Moreover, the upregulation of germin-like protein genes we observed aligns with reports in peanut, grapevine, and other species, where GLPs are linked to stress responses and developmental regulation (Godfrey *et al*. 2007; Liao *et al*. 2021; Yang *et al*. 2023b).

4.2. KEGG Pathway Enrichment

Pathway enrichment analysis provided additional context to the observed transcriptomic changes in the long-juvenile (LJ) soybean line. Several key pathways were significantly enriched for down-regulated genes, including ribosome biogenesis, zeatin biosynthesis, isoflavonoid biosynthesis, biosynthesis of various secondary plant metabolites, and MAPK signaling. The repression of ribosome biogenesis suggests a reduction in protein synthesis capacity, which is consistent with previous studies showing that ribosomal activity is tightly coordinated with growth rates and developmental timing in plants (Byrne 2009; Weis *et al.* 2015). Downregulation of zeatin biosynthesis suggests a reduction in cytokinin-related developmental signals. Since cytokinins are central regulators of cell division, meristem activity, and floral induction (Werner *et al*. 2001; Sakakibara 2020), their reduced activity in LJ plants may contribute to delayed flowering and extended vegetative growth. Similarly, suppression of MAPK signaling cascades suggests a dampening of stress- and hormone-mediated signaling, which has been implicated in both flowering regulation and adaptation to environmental cues (He *et al*. 2020).

In contrast, several pathways were significantly enriched for upregulated genes, including photosynthesis, starch and sucrose metabolism, fatty acid metabolism, and motor protein-related processes. These findings indicate that, although individual photosynthesis-related genes such as psbZ and psbD were down-regulated, the broader enrichment pattern reflects a coordinated up-regulation of other photosynthetic and energy metabolism components. This apparent discrepancy underscores the distinction between single-gene differential expression and pathway-level analysis, where collective modest changes across multiple genes can outweigh the strong down-regulation of a few key genes (Khatri *et al*. 2012). The up-regulation of sugar and lipid metabolism is consistent with enhanced carbon assimilation and energy storage during prolonged vegetative growth. At the same time, enrichment of motor protein pathways reflects increased cellular transport and cytoskeletal activity, supporting active growth.

Overall, the enrichment results suggest that the LJ line undergoes a reprogramming of its transcriptome,

characterized by the down-regulation of pathways linked to developmental progression (ribosome biogenesis, cytokinin biosynthesis, and MAPK signaling) and the up-regulation of energy-producing and metabolic pathways (photosynthesis, sugar, and lipid metabolism). This dual shift may underlie the extended juvenile phase, favoring resource accumulation and vegetative vigor prior to the floral transition.

4.3. Expression Patterns of Flowering Time Regulators

Analysis of key flowering time genes, previously identified as associated with the long juvenile trait, revealed discrete differences in expression. The flowering repressor gene FT2A (E9) showed a modest reduction in expression in the AP18 line, consistent with its function in delaying flowering (Kong *et al*. 2018). This supports the hypothesis that reduced FT2A expression contributes to the LJ phenotype through delaying floral transition.

Interestingly, ELF3 (J) transcripts were slightly greater in AP18, although the j allele has been linked to loss-of-function mutations that disrupt protein activity rather than transcript abundance (Lu *et al*. 2017; Fang *et al*. 2019). This suggests that post-transcriptional or post-translational control, rather than mRNA abundance, may be the cause of the functional breakdown of ELF3 in LJ lines, highlighting the complexity of flowering time regulation.

Analysis of flowering time regulators revealed modest expression changes that support the LJ phenotype. FT2A (E9) exhibited a modest reduction in the AP18 line (as shown in Kong *et al*. 2018), consistent with studies demonstrating that allele-specific repression of FT2A delays flowering in soybean and other legumes (Cai *et al*. 2024). In a similar context, combined mutations in FT2A and FT5A significantly delay flowering time, enhance vegetative growth, and increase yield, reinforcing the role of FT2A repression in prolonging juvenility (Cai *et al*. 2017).

Meanwhile, ELF3 (J) transcript levels were slightly elevated in AP18, which aligns with reports showing that loss-of-function mutations in GmELF3a impair protein function without suppressing mRNA expression, pointing to post-transcriptional or post-translational regulation (Fang *et al*. 2020). This highlights the multi-layered control of ELF3 activity within the Flowering Pathway Complex and its impact on the LJ trait.

4.4. Biological Significance and Future Directions

The integrative transcriptomic and pathway analyses provide new insights into the molecular basis of the long-juvenile (LJ) trait in soybean. A central feature of the LJ line is the strong down-regulation of photosynthesis-related proteins, ribosomal components, and genes involved in sugar and lipid transport. However, at molecular pathway levels, photosynthetic, ribosome biogenesis, sugar, and lipid metabolic pathways were enriched with upregulated genes. Altogether, this observation suggests a strategic reduction in primary metabolic activity and translational capacity. In contrast, germin-like proteins (GLPs) and pathways associated with secondary metabolism were upregulated, indicating enhanced stress defense and developmental buffering. Similar GLP induction has been implicated in enhancing tolerance to oxidative stress and pathogen pressure, thereby supporting survival under extended vegetative phases (Govindan *et al*. 2024).

These molecular reorganizations align with the delayed flowering and prolonged vegetative growth observed in LJ soybeans. The suppression of energy-intensive processes, such as photosynthesis and ribosome biogenesis, may reflect a resource reallocation strategy. At the same time, the activation of defense- and signaling-related genes could help stabilize the juvenile state. Such trade-offs between growth, development, and defense are increasingly recognized as central themes in plant adaptation (Horiguchi *et al*. 2012; Xu *et al*. 2023).

Future work should focus on functional validation of candidate genes highlighted in this study. Time-series transcriptomics and proteomics will be valuable to capture dynamic transitions in gene expression across developmental stages. Functional assays (e.g., CRISPR knockouts or overexpression lines) targeting GLPs or key secondary metabolism regulators could help clarify their causal roles in maintaining the LJ phenotype, and in addition, integrating epigenetic profiling and small RNA analyses (e.g., the miR156–SPL module) may reveal how post-transcriptional and chromatin-level regulation contribute to flowering time and juvenility in soybean (Wu *et al*. 2009; Cao *et al*. 2015; Huang *et al.* 2024).

By combining these approaches, future research can transition from descriptive transcriptomics to a mechanistic understanding, ultimately enabling the targeted manipulation of juvenile traits for soybean breeding.

In conclusion, This research presents a comprehensive transcriptomic analysis comparing the long juvenile soybean line AP18 with the Grobogan control cultivar. The analysis reveals distinctive gene expression signatures and pathway modulations associated with the long juvenile phenotype, including the downregulation of some photosynthetic and ribosomal genes, alongside the upregulation of genes encoding defence-related germin-like proteins. Differential expression of key flowering regulators, most notably FT2A (E9) and ELF3 (J), provides molecular insights consistent with their putative role in regulating flowering time, although the complexity of their regulation requires further elucidation. Together, these findings enhance our understanding of the molecular foundations of the long juvenile trait in soybean and highlight key targets for breeding initiatives aimed at improving crop adaptability and yield.

Acknowledgements

This study was funded by RIIM Batch 3 of BRIN-LPDP (2023-2025), Contract Numbers B-846/II.7.5/FR.06/5/2023 and B-861/III.11/FR.06/5/2023. We thank Rosliana Purwaning Dyah, Ratna Utari, and Dani Satyawan for their assistance with fieldwork and thoughtful discussions. Bioinformatics work was facilitated by the Mahameru High Performance Computing Facility of the National Research and Innovation Agency, Republic of Indonesia (BRIN).

References

Byrne, M.E., 2009. A role for the ribosome in development. *Trends in Plant Science*. 14, 512-519. https://doi.org/10.1016/j.tplants.2009.06.009

Cai, Y., Chen, L., Liu, X., Guo, C., Sun, S., Wu, C., Jiang, B., Han, T., & Hou, W., 2017. CRISPR/Cas9-mediated targeted mutagenesis of GmFT2a delays flowering time in soya bean. *Plant Biotechnology Journal*. 16, 176-185. https://doi.org/10.1111/pbi.12758

Cai, Y., Chen, L., Liu, X., Yao, W., & Hou, W., 2024. GmNF-YC4 delays soybean flowering and maturation by directly repressing GmFT2a and GmFT5a expression. *Journal of Integrative Plant Biology*. 66, 1370-1384. https://doi.org/10.1111/jipb.13668

Cao, D., Li, Y., Wang, J., Nan, H., Wang, Y., Lu, S., Jiang, Q., Li, X., Shi, D., Fang, C., Yuan, X., Zhao, X., Li, X., Liu, B., & Kong, F., 2015. GmmiR156b overexpression delays flowering time in soybean. *Plant Molecular Biology*. 89, 353-363. https://doi.org/10.1007/s11103-015-0371-5

Cao, D., Takeshima, R., Zhao, C., Liu, B., Jun, A., & Kong, F., 2016. Molecular mechanisms of flowering under long days and stem growth habit in soybean. *Journal of Experimental Botany*. 73, 2399-2412. https://doi.org/10.1093/jxb/erw394

Chen, S., Zhou, Y., Chen, Y., & Gu, J., 2018. fastp: An ultra-fast all-in-one FASTQ preprocessor. *Bioinformatics*. 34, i884-i890. https://doi.org/10.1093/bioinformatics/bty560

Deng, Z.-L., Münch, P.C., Mreches, R., & McHardy, A.C., 2022. Rapid and accurate identification of ribosomal RNA sequences via deep learning. *Nucleic Acids Research*. 50, e60-e60. https://doi.org/10.1093/nar/gkac112

Dobin, A., Davis, C.A., Schlesinger, F., Drenkow, J., Zaleski, C., Jha, S., Batut, P., Chaisson, M., & Gingeras, T.R., 2012. STAR: Ultrafast universal RNA-seq aligner. *Bioinformatics*. 29, 15-21. https://doi.org/10.1093/bioinformatics/bts635

Fang, C., Chen, L., Nan, H., Kong, L., Li, Y., Zhang, H., Li, H., Li, T., Tang, Y., Hou, Z., Dong, L., Cheng, Q., Lin, X., Zhao, X., Yuan, X., Liu, B., Kong, F., & Lu, S., 2019. Rapid identification of consistent novel QTLs underlying long-juvenile trait in soybean by multiple genetic populations and genotyping-by-sequencing. *Molecular Breeding*. 39. https://doi.org/10.1007/s11032-019-0979-2

Fang, X., Han, Y., Liu, M., Jiang, J., Li, X., Lian, Q., Xie, X., Huang, Y., Ma, Q., Nian, H., Qi, J., Yang, C., & Wang, Y., 2020. Modulation of evening complex activity enables north-to-south adaptation of soybean. *Science China Life Sciences*. 64, 179-195. https://doi.org/10.1007/s11427-020-1832-2

Fattah, A., Idaryani., Herniwati., Yasin, M., Suriani, S., Salim., Nappu, M.B., Mulia, S., Irawan., Hannan, M.F., Wulanningtyas, H.S., Saenong, S., Dewayani, W., Suriany., Winanda, E., Manwan, S.W., Asaad, M., Warda., Nurjanani., Nurhafsah., Gaffar., Sunanto, A., Fadwiwati., Nurdin, A.Y., Dahya, M., Ella, A., 2024. Performance and morphology of several soybean varieties and responses to pests and diseases in South Sulawesi. *Heliyon*. 10, e25507. https://doi.org/10.1016/j.heliyon.2024.e25507

Godfrey, D., Able, A.J., & Dry, I.B., 2007. Induction of a Grapevine Germin-Like Protein (VvGLP3) Gene Is Closely Linked to the Site of Erysiphe necator Infection: A Possible Role in Defense?. Molecular Plant-Microbe Interactions. 20, 1112-1125. https://doi.org/10.1094/mpmi-20-9-1112

Gong, Z., 2020. Flowering phenology as a core domestication trait in soybean. *Journal of Integrative Plant Biology*. 62, 546-549. https://doi.org/10.1111/jipb.12934

Govindan, G., Sandhiya, K.R., Alphonse, V., & Somasundram, S., 2024. Role of germin-like proteins (GLPs) in biotic and abiotic stress responses in major crops: A review on plant defense mechanisms and stress tolerance. *Plant Molecular Biology Reporter*. 42, 450-468. https://doi.org/10.1007/s11105-024-01434-9

Han, X., Xu, Z.-R., Zhou, L., Han, C.-Y., & Zhang, Y.-M., 2021. Identification of QTNs and their candidate genes for flowering time and plant height in soybean using multi-locus genome-wide association studies. *Molecular Breeding*. 41, 39. https://doi.org/10.1007/s11032-021-01230-3

Hartwig, E.E., & Kiihl, R.A.S., 1979. Identification and utilization of a delayed flowering character in soybeans for short-day conditions. *Field Crops Research*. 2, 145-151. https://doi.org/10.1016/0378-4290(79)90017-0

He, X., Wang, C., Wang, H., Li, L., & Wang, C., 2020. The function of MAPK cascades in response to various stresses in horticultural plants. *Frontiers in Plant Science*. 11, 952. https://doi.org/10.3389/fpls.2020.00952

Horiguchi, G., Van Lijsebettens, M., Candela, H., Micol, J.L., & Tsukaya, H., 2012. Ribosomes and translation in plant developmental control. *Plant Science*. 191-192, 24-34. https://doi.org/10.1016/j.plantsci.2012.04.008

Huang, X., Wang, Y., Zhang, S., Pei, L., You, J., Long, Y., Li, J., Zhang, X., Zhu, L., & Wang, M., 2024. Epigenomic and 3D genomic mapping reveals developmental dynamics and subgenomic asymmetry of transcriptional regulatory architecture in allotetraploid cotton. *Nature Communications*. 15, 10721. https://doi.org/10.1038/s41467-024-55309-4

Kanehisa, M., Furumichi, M., Sato, Y., Kawashima, M., & Ishiguro-Watanabe, M., 2022. KEGG for taxonomy-based analysis of pathways and genomes. *Nucleic Acids Research*. 51, D587-D592. https://doi.org/10.1093/nar/gkac963

Khatri, P., Sirota, M., & Butte, A.J., 2012. Ten years of pathway analysis: Current approaches and outstanding challenges. *PLoS Computational Biology*. 8, e1002375. https://doi.org/10.1371/journal.pcbi.1002375

Kong, L., Lu, S., Wang, Y., Fang, C., Wang, F., Nan, H., Su, T., Li, S., Zhang, F., Li, X., Zhao, X., Yuan, X., Liu, B., & Kong, F., 2018. Quantitative trait locus mapping of flowering time and maturity in soybean using next-generation sequencing-based analysis. *Frontiers in Plant Science*. 9, 995. https://doi.org/10.3389/fpls.2018.00995

Li, H., Chen, Z., Wang, F., Xiang, H., Liu, S., Gou, C., Fang, C., Chen, L., Bu, T., Kong, F., Zhao, X., Liu, B., & Lin, X., 2024. J-family genes redundantly regulate flowering time and increase yield in soybean. *The Crop Journal*. 12, 944-949. https://doi.org/10.1016/j.cj.2024.03.013

Liao, L., Hu, Z., Liu, S., Yang, Y., & Zhou, Y., 2021. Characterization of germin-like proteins (GLPs) and their expression in response to abiotic and biotic stresses in cucumber. *Horticulturae*. 7, 412. https://doi.org/10.3390/horticulturae7100412

Love, M.I., Huber, W., & Anders, S., 2014. Moderated estimation of fold change and dispersion for RNA-seq data with DESeq2. *Genome Biology*. 15, 550. https://doi.org/10.1186/s13059-014-0550-8

Lu, S., Zhao, X., Hu, Y., Liu, S., Nan, H., Li, X., Fang, C., Cao, D., Shi, X., Kong, L., Su, T., Zhang, F., Li, S., Wang, Z., Yuan, X., Cober, E. R., Weller, J. L., Liu, B., Hou, X., Tian, Z., & Kong, F., 2017. Natural variation at the soybean *J locus* improves adaptation to the tropics and enhances yield. *Nature Genetics*. 49, 773-779. https://doi.org/10.1038/ng.3819

Lu, S., Dong, L., Fang, C., Liu, S., Kong, L., Cheng, Q., Chen, L., Su, T., Nan, H., Zhang, D., Zhang, L., Wang, Z., Yang, Y., Yu, D., Liu, X., Yang, Q., Lin, X., Tang, Y., Zhao, X., Yang, X., Tian, C., Xie, Q., Li, X., Yuan, X., Tian, Z., Liu, B., Weller, J. L., & Kong, F., 2020. Stepwise selection on homeologous PRR genes controlling flowering and maturity during soybean domestication. *Nature Genetics*. 52, 428-436. https://doi.org/10.1038/s41588-020-0604-7

Lv, T., Wang, L., Zhang, C., Liu, S., Wang, J., Lu, S., Fang, C., Kong, L., Li, Y., Li, Y., Hou, X., Liu, B., Kong, F., & Li, X., 2022. Identification of two quantitative genes controlling soybean flowering using bulked-segregant analysis and genetic mapping. *Frontiers in Plant Science*. 13, 987073. https://doi.org/10.3389/fpls.2022.987073

Morgan, M., & Shepherd, L., 2024. AnnotationHub: Client to access AnnotationHub resources. https://bioconductor.org/packages/AnnotationHub [Date accessed: 2 May 2025].

Mortazavi, A., Williams, B.A., McCue, K., Schaeffer, L., & Wold, B., 2008. Mapping and quantifying mammalian transcriptomes by RNA-Seq. *Nature Methods*. 5, 621-628. https://doi.org/10.1038/nmeth.1226

Ritchie, M.E., Phipson, B., Wu, D., Hu, Y., Law, C.W., Shi, W., & Smyth, G.K., 2015. limma powers differential expression analyses for RNA-sequencing and microarray studies. *Nucleic Acids Research*. 43, e47-e47. https://doi.org/10.1093/nar/gkv007

Robinson, M.D., McCarthy, D.J., & Smyth, G.K., 2009. edgeR: A Bioconductor package for differential expression analysis of digital gene expression data. *Bioinformatics*. 26, 139-140. https://doi.org/10.1093/bioinformatics/btp616

Sakakibara, H., 2020. Cytokinin biosynthesis and transport for systemic nitrogen signaling. *The Plant Journal*. 105, 421-430. https://doi.org/10.1111/tpj.15011

Schmutz, J., Cannon, S.B., Schlueter, J., Ma, J., Mitros, T., Nelson, W., Hyten, D.L., Song, Q., Thelen, J.J., Cheng, J., Xu, D., Hellsten, U., May, G.D., Yu, Y., Sakurai, T., Umezawa, T., Bhattacharyya, M.K., Sandhu, D., Valliyodan, B., Lindquist, E., Peto, M., Grant, D., Shu, S., Goodstein, D., Barry, K., Futrell-Griggs, M., Abernathy, B., Du, J., Tian, Z., Zhu, L., Gill, N., Joshi, T., Libault, M., Sethuraman, A., Zhang, X.-C., Shinozaki, K., Nguyen, H.T., Wing, R.A., Cregan, P., Specht, J., Grimwood, J., Rokhsar, D., Stacey, G., Shoemaker, R.C., & Jackson, S.A., 2010. Genome sequence of the palaeopolyploid soybean. *Nature*. 463, 178-183. https://doi.org/10.1038/nature08670

Schubert, M., Lindgreen, S., & Orlando, L., 2016. Adapter Removal v2: Rapid adapter trimming, identification, and read merging. *BMC Research Notes*. 9, 1-7. https://doi.org/10.1186/s13104-016-1900-2

Soehendi, R., Suhartina, Mejaya, M.J., Purwantoro., Trustinah., & Nuryati., 2024. Breeding of drought tolerant soybean varieties adaptable to rainfed area of Indonesia. *AIP Conference Proceedings*. 3001, 030016. https://doi.org/10.1063/5.0184506

Suhartina., Purwantoro., Nugraheni, N., Taufiq, A., & Mejaya, M.J., 2022. Yield stability performance of soybean (*Glycine max* [L.] Merrill) lines tolerant to drought. *AIP Conf. Proc*. 2462, 020004. https://doi.org/10.1063/5.0075158

Tasma, I.M., Lorenzen, L., Green, D. & Shoemaker, R.C., 2001. Mapping genetic loci for flowering time, maturity, and photoperiod insensitivity in soybean. *Molecular Breeding*. 8, 25-35. https://doi.org/10.1023/A:1011998116037

Tasma, I.M. & Shoemaker, R.C., 2003. Mapping flowering time gene homologs in soybean and their association with maturity (E) loci. *Crop Science*. 43, 319-328. https://doi.org/10.2135/cropsci2003.3190

Tasma, I.M., Yani, N.P.M.G., Purwaningdyah, R., Satyawan, D., Nugroho, K., Lestari, P., Trijatmiko, K.R., & Mastur, M., 2018. Genetic diversity analysis and F2 population development for breeding of long juvenile trait in soybean. *Jurnal AgroBiogen*. 14, 11-22. https://doi.org/10.21082/jbio.v14n1.2018.p11-22

Utomo, F.H., Kristanto, B.A., & Kusmiyati, F., 2018. Persilangan 4 varietas kedelai (*Glycine max* L.) dalam rangka perakitan kedelai tahan kering. *Journal of Agro Complex*. 2, 93. https://doi.org/10.14710/joac.2.2.93-101

Wang, L., Wang, S., & Li, W., 2012. RSeQC: Quality control of RNA-seq experiments. *Bioinformatics*. 28, 2184-2185. https://doi.org/10.1093/bioinformatics/bts356

Wang, J., Wang, H., Deng, T., Liu, Z., & Wang, X., 2019. Time-coursed transcriptome analysis identifies key expressional regulation in growth cessation and dormancy induced by short days in Paulownia. *Scientific Reports*. 9, 16602. https://doi.org/10.1038/s41598-019-53283-2

Weis, B.L., Kovacevic, J., Missbach, S., & Schleiff, E., 2015. Plant-Specific features of ribosome biogenesis. *Trends in Plant Science*. 20, 729-740. https://doi.org/10.1016/j.tplants.2015.07.003

Werner, T., Motyka, V., Strnad, M., & Schmülling, T., 2001. Regulation of plant growth by cytokinin. *Proceedings of the National Academy of Sciences*. 98, 10487-10492. https://doi.org/10.1073/pnas.171304098

Wu, G., Park, M.Y., Conway, S.R., Wang, J.-W., Weigel, D., & Poethig, R.S., 2009. The sequential action of miR156 and miR172 regulates developmental timing in *Arabidopsis*. *Cell*. 138, 750-759. https://doi.org/10.1016/j.cell.2009.06.031

Wu, F., Kang, X., Wang, M., Haider, W., Price, W.B., Hajek, B., & Hanzawa, Y., 2019. Transcriptome-Enabled network inference revealed the gmcol1 feed-forward loop and its roles in photoperiodic flowering of soybean. *Frontiers in Plant Science*. 10, 1221. https://doi.org/10.3389/fpls.2019.01221

Xu, Y., Song, D., Qi, X., Asad, M., Wang, S., Tong, X., Jiang, Y., & Wang, S., 2023. Physiological responses and transcriptome analysis of soybean under gradual water deficit. *Frontiers in Plant Science*. 14, 1269884. https://doi.org/10.3389/fpls.2023.1269884

Yang, Q., Sharif, Y., Zhuang, Y., Chen, H., Zhang, C., Fu, H., Wang, S., Cai, T., Chen, K., Raza, A., Wang, L., & Zhuang, W., 2023b. Genome-wide identification of germin-like proteins in peanut (*Arachis hypogea* L.) and expression analysis under different abiotic stresses. *Frontiers in Plant Science*. 13, 1044144. https://doi.org/10.3389/fpls.2022.1044144

Yue, Y., Jiang, Z., Sapey, E., Wu, T., Sun, S., Cao, M., Han, T., Li, T., Nian, H., & Jiang, B., 2021. Transcriptomal dissection of soybean circadian rhythmicity in two geographically, phenotypically and genetically distinct cultivars. *BMC Genomics*. 22, 529. https://doi.org/10.1186/s12864-021-07869-8

Zhang, J., Huang, D., Zhao, X., & Zhang, M., 2021. Evaluation of drought resistance and transcriptome analysis for the identification of drought-responsive genes in *Iris germanica*. *Scientific Reports*. 11, 16308. https://doi.org/10.1038/s41598-021-95633-z